International Journal of Technical Research and Applications e-ISSN: 2320-8163,
www.ijtra.com Volume 4, Issue 3 (May-June, 2016), PP. 468-473

PERFORMANCE ANALYSIS OF SMART GRID WITH SUPER CONDUCTING FAULT CURRENT LIMITER IN A SOLAR AND WIND BASED MICROGRID

Avinash Chougule[1], Dr. S. G. Kanade[2]
[1]ME Student, [2]Professor
Department of Electrical Engineering
Tssm's bhivarabai sawant college of engineering and research, narhe
Pune - 411 041
mehta.hrishi@gmail.com

***Abstract*— Today due to competitiveness in the energy market, increasing number of power generators are being interconnected with the main grid. This in turn increases the level of fault current in the system. In general, circuit breakers used today have delay of about two to three typical cycles in responding to the trip command from the relay. This paper describes resistive Super Conducting Fault Current Limiter (SFCL) as an innovative equipment which has the capability to reduce this fault current level in its first cycle of fault current. The model is implemented using MATLAB SimPowerSystem and uses a resistive type SFCL which act like a controllable resistor. All line faults have been simulated at different locations in the test system consisting of a 10MVA wind power system and 50kW solar power system and the effect of the SFCL and its location on the fault current at point of common coupling is observed. The paper concludes with results showing the optimal connection for SFCL in the test system.**

Keywords—SFCL, PCC, Wind Farm, Solar Farm, MPPT, Distributed Generation, Fault Current Limiter, HTS

I. INTRODUCTION

Fault levels in today's power systems have increased beyond traditional limits. Old devices like higher impedance transformers, split bus bars and fuses have started failing against these levels. Increasing the limiting capacity of these devices not only require capital cost but also increase the level of loss in the system. Also reliability of the complete system gets compromised due to constant excessive stress on the system. A high-temperature superconductor (HTS) is seen as an alternative to this problem. It has the ability to improve transient performance of the system in fast and effective manner. There were a few researches based on its applicability but they haven't been tested to focus on real system problems and the application of SFCL for real application system have been selected as the topic of interest for this paper.

After rigorous literature survey and trials on various test systems, important factors that need to be considered for practical implementation of SFCL can be high:

1) Optimal place to install the SFCL;

2) Optimal resistive value of the SFCL connected in series with a transmission line during a short-circuit fault;

3) Potential protection-coordination problem with other existing protective devices such as a recloser and a circuit breaker.

Keeping these factors in mind, the effect of SFCL and its feasible position in micro-grid was investigated considering a wind farm and solar farm integrated with a distribution grid model as one of typical configurations of the smart grid. The impacts of SFCL on the wind farm and solar farm and the strategic location of SFCL in a micro grid which limits fault current from all power sources and has no negative effect on the integrated wind farm is suggested in this paper.

The paper is organized as follows. Section II covers the concept of SFCL along with its mathematical model. Section III discussed the PV and Wind farm system used for study in this work. System Model is described in section IV. Section V deals with results obtained from the simulation study and Section VI concludes the paper highlighting the contributions of the paper.

II. CONCEPT AND MODELLING OF SFCL

Fault current limiters (FCLs) are developed to overcome problems. An ideal FCL should have the following characteristics:

a) Zero impedance in the normal operation;
b) No power loss in the normal operation;
c) Large impedance in the fault conditions;
d) Quick appearance of impedance when the fault occurs;
e) Fast recovery after fault removal [6].

Resistive SFCLs utilize the superconducting material as the main current carrying conductor under normal grid operation [13]. The superconductive shunt with resistive bypass is shown in Fig. 1. In this case the bypass element limits the current during fault. The fault current is limited when it is more than the critical current of the superconductor element and it operates in high resistance state which limits the fault current. Superconductor material of high resistivity in its non-superconductor state is preferred as it will limit the current during fault. During normal operation the R2 is zero and when there is fault, resistance R2 becomes very high which limits the current during fault. The resistance R is the

bypass resistance. During fault the fault current is transferred from resistance R2 to R [14].

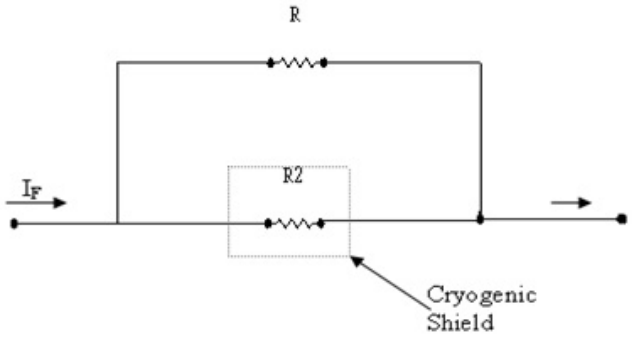

Fig. 1. Superconductor Fault Current Limiter, Resistive Shunt type

The flowchart and operating characteristics of the same can be seen in Fig. 2 and 3. Fig. 3 interprets quenching and recovery characteristics of the SFCL. It is clear from Fig. 3 that at normal operating condition impedance of SFCL is zero. But when fault takes place at t = t0, quenching progression starts and then impedance goes to its peak value. After recovery of fault impedance again goes back to zero at t = t3.

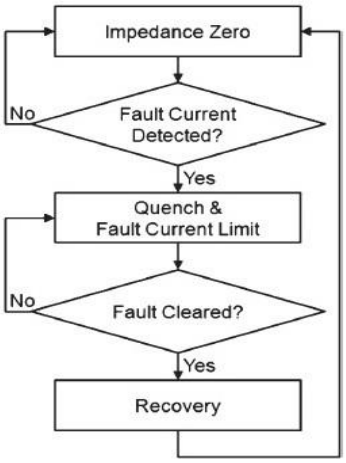

Fig. 2. Operating Principle Representation in Flowchart

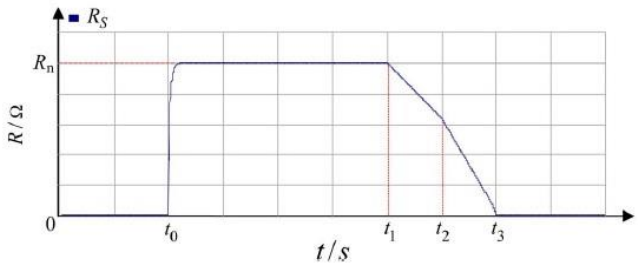

Fig. 3. Quench and Recovery characteristics of SFCL

Mathematical Model of SFCL

Mathematical model of SFCL is represented as a equation of non-linear resistance showing its non-linearity in different temperature zones as given in the following equation.

$$R(t)= \begin{cases} 0 & (t < t_0) \\ R_n[1-\exp\left(-\frac{t-t_0}{T}\right)]^{1/2} & (t_0 \le t < t_1) \\ a_1(t-t_{1)} + b_1 & (t_1 \le t < t_2) \\ a_2(t-t_{2)} + b_2 & (t_2 \le t < t_3) \\ 0 & (t \ge t_3) \end{cases} \quad (1)$$

Where

R_n = Impedance being saturated at normal temp.

τ = time constant of transition from the superconducting state to the normal state

t_0, t_1, t_2, t_3= quench starting time, first recovery starting time, second recovery starting time & third recovery starting time

a_1, a_2, b_1, b_2 = coefficient of finite linear function.

III. Modelling of PV System and Wind Farm

As the world discovers new ways to meet its growing energy needs, energy generated from Sun, which is better known as solar power and energy generated from wind called the wind power are being considered as a means of generating power. These energy sources will define the future of energy scenario.

A) Wind Farm

The Matlab model is based on the steady-state power characteristics of the turbine. The stiffness of the drive train is infinite and the friction factor and the inertia of the turbine must be combined with those of the generator coupled to the turbine. The output power of the turbine is given by the following equation.

$P_m = c_p(\gamma,\beta)\ \rho A/2\ v^3_{wind}$ (2)

where

Pm is Mechanical output power of the turbine (W)

c_p is Performance coeffcient of the turbine

ρ is Air density (kg/m^3)

A is Turbine swept area (m^2)

v_{wind} is Wind speed (m/s)

γ is Tip speed ratio of the rotor blade tip speed to wind speed

β is Blade pitch angle (deg).

The mechanical power and the stator electric power output are computed as follows:

$P_m = T_m \omega_r$

$P_s = T_{em} \omega_s$

For a lossless generator the mechanical equation is:

$J\, d\omega_r/dt = T_m - T_{em}$ (3)

In steady-state at fixed speed for a lossless generator $T_m = T_{em}$ and $P_m = P_s + P_r$.

It follows that

$P_r=P_m - P_s=T_m \omega_r - T_{em} \omega_s=-T_m[(\omega_s - \omega_r)/\omega_s]\omega_s=-sT_m\omega_s=-sP_s$ (4)

where s is defined as slip of the generator: $s=(\omega_s - \omega_r)/\omega_s$.

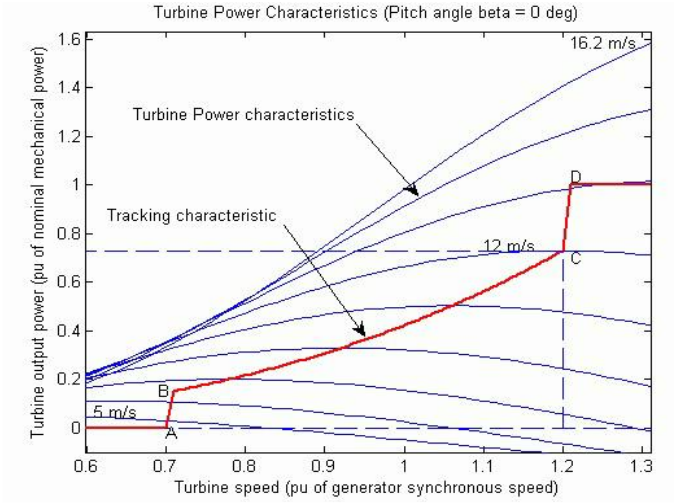

Fig. 4. Turbine Characteristics and Tracking Characteristic

The power is controlled in order to follow a pre-defined power-speed characteristic, named tracking characteristic. An example of such a characteristic is illustrated in Fig. 4, by the ABCD curve superimposed to the mechanical power characteristics of the turbine obtained at different wind speeds. Fig. 5 shows MATLAB implementation of a 10MW Wind Farm system.

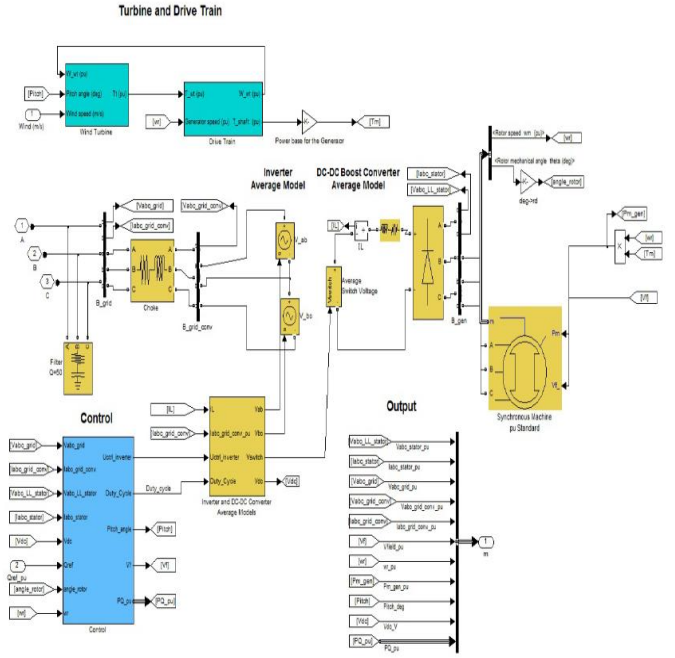

Fig. 5. MATLAB implementation of Wind Farm

B) Photovoltaic System

A typical solar farm consists of an string or array of solar panels connected in series parallel combination to produce sufficient power at specified voltage and current ratings. These panels produce dc voltage which is then converted into ac by use of an inverter. The traditional equivalent circuit of a solar cell represented by a current source in parallel with one diode is shown in Fig. 6 and its electrical characteristics are shown in Fig. 7.

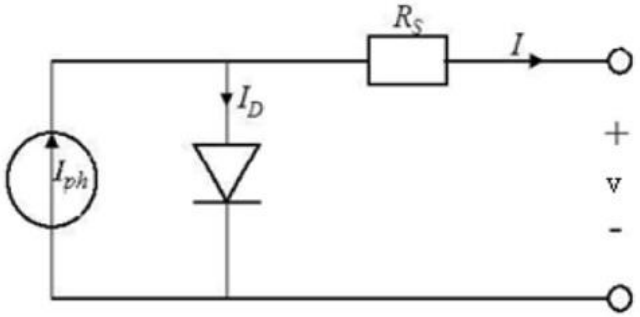

Fig. 6. PV Cell

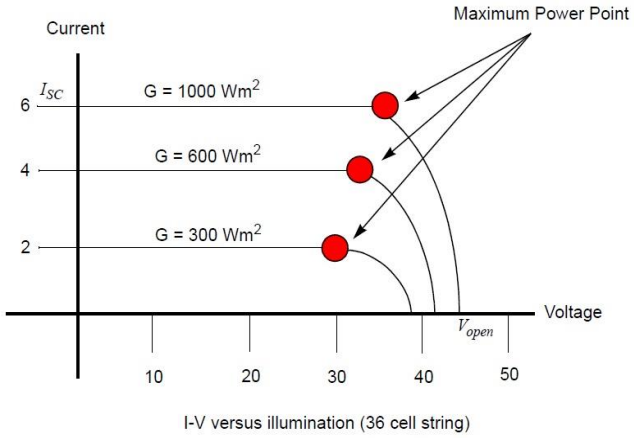

Fig. 7. PV Module Electrical Characteristics

The single-diode model includes four components: a photo current source, a diode parallel to the source, a series resistor R, and a shunt resistor Rp. Its mathematical model can be expressed as

$$I = Iph - Isat\{\exp[q(V + IRs)/(AKT)] - 1\} \quad (5)$$

where
I is current from solar panel
Iph is the Photo current of solar cell
Isat is the Reverse saturation current
q is Electronic charge
A is A dimensionless factor
K is Boltzmann constant
T is Temperature (in Kelvin)
V is the output voltage of the cell
Rs is series resistance.

Eqn (5) shows that the output characteristic of a solar cell is nonlinear and vitally affected by solar radiation, temperature, and load condition.

MPPT Control

The MPP voltage range for these PV modules is normally defined in the range from 27V to 45V, at a power generation

of approximate 200W, and their open- circuit voltage is below 45V. In order to capture the maximum energy from the PV module, solar inverters must guarantee that the PV module is operated at the MPP. This is accomplished by the maximum power point control loop known as the Maximum Power Point Tracker (MPPT). Many MPPT algorithms have been proposed in the literature, out of which perturbation and observation (P&O) method is used in this work as it only requires two sensors, which results in a reduction of hardware requirements and cost. Therefore, the P&O method is used to control the MPPT process and is shown in flowchart in Fig. 8. As PV voltage and current are determined, the power is calculated. At the maximum power point, the derivative (dP=dV) is equal to zero. The maximum power point can be achieved by changing the reference voltage by the amount of ΔVref.

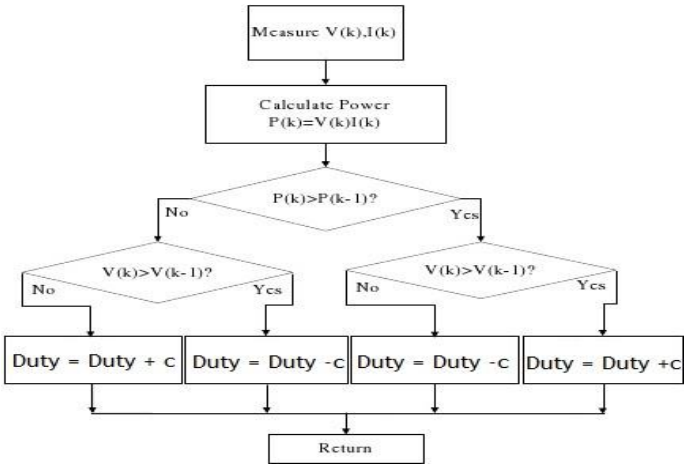

Fig. 8. P&O Flowchart

Matlab implementation of solar panel with MPPT algorithm is shown in Fig. 9. The model consists of PV array, buck-boost converter and a MPPT algorithm. The panel array is designed to be of 50kW rating.

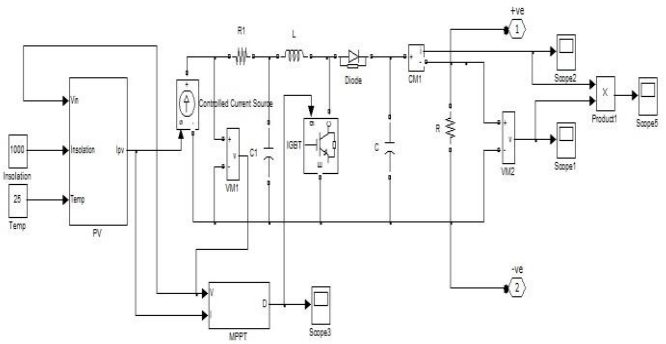

Fig. 9. Matlab Model of a Solar Panel with buck-boost converter and MPPT

IV. SYSTEM UNDER STUDY

A) MATLAB Implementation of Resistive SFCL

The three phase resistive type SFCL was modeled considering four fundamental parameters of a resistive type SFCL. These parameters and their selected values are:
Switching time = 2 msec.
Minimum impedance = 0.01 Ohms.
Maximum impedance = 20 Ohms.
Actuating current =550 A.
Recovery time = 10 msec.
Working voltage = 22.9 kv.

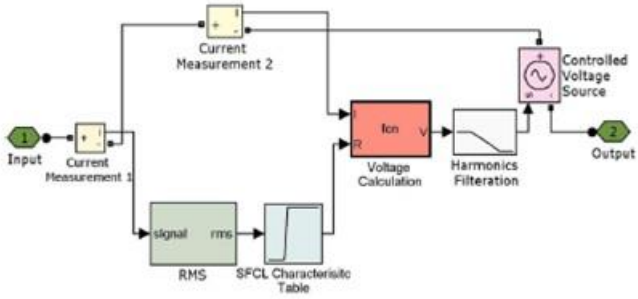

Fig. 10. SFCL model developed in Simulink/Sim- PowerSystem.

Fig. 10 shows the SFCL model developed in Simulink/Sim-PowerSystem. The SFCL model works as follows. First, SFCL model calculates the RMS value of the passing current and then compares it with the characteristic table. Second, if a passing current is larger than the triggering current level, SFCLs resistance increases to maximum impedance level in a pre-defined response time. Finally, when the current level falls below the triggering current level the system waits until the recovery time and then goes into normal state.The modeled power system was based on Korean electric transmission and distribution power system [4]. Newly developed micro grid model was designed by integrating a 10 MVA wind farm with the distribution network. Fig. 11 shows the power system m odel designed in Simulink / Sim-Power-System. The power system is composed of a 100 MVA conventional power plant, composed of 3-phase synchronous machine, connected with 200 km long 154 kV distributed-parameters transmission line through a step-up transformer TR1. At the substation (TR2), voltage is stepped down to 22.9 kV from 154 kV. High power industrial load (6 MW) and low power domestic loads (1 MW each) are being supplied by separate distribution branch networks. The wind farm is directly connected with the branch network (B1) through transformer TR3 and is providing power to the domestic loads. The 10 MVA wind farm is composed of five fixed-speed induction-type wind turbines each having a rating of 2MVA. At the time of fault, the domestic load is being provided with 3 MVA out of which 2.7 MVA is being provided by the wind farm. In Figure 11 artificial fault and locations of SFCL are indicated in the diagram. Three kinds of fault points are marked as Fault 1, Fault 2 and Fault 3, which represent three-phase-to-ground faults in distribution grid, customer grid and transmission line respectively.

Four prospective locations for SFCL installation are marked as

- Location 1 (Substation)
- Location 2 (Branch Network)
- Locations 3 (Wind farm integration point with the grid)
- Location 4 (Wind Farm).

Generally, conventional fault current protection devices are located in Location one (1) and Location two (2).

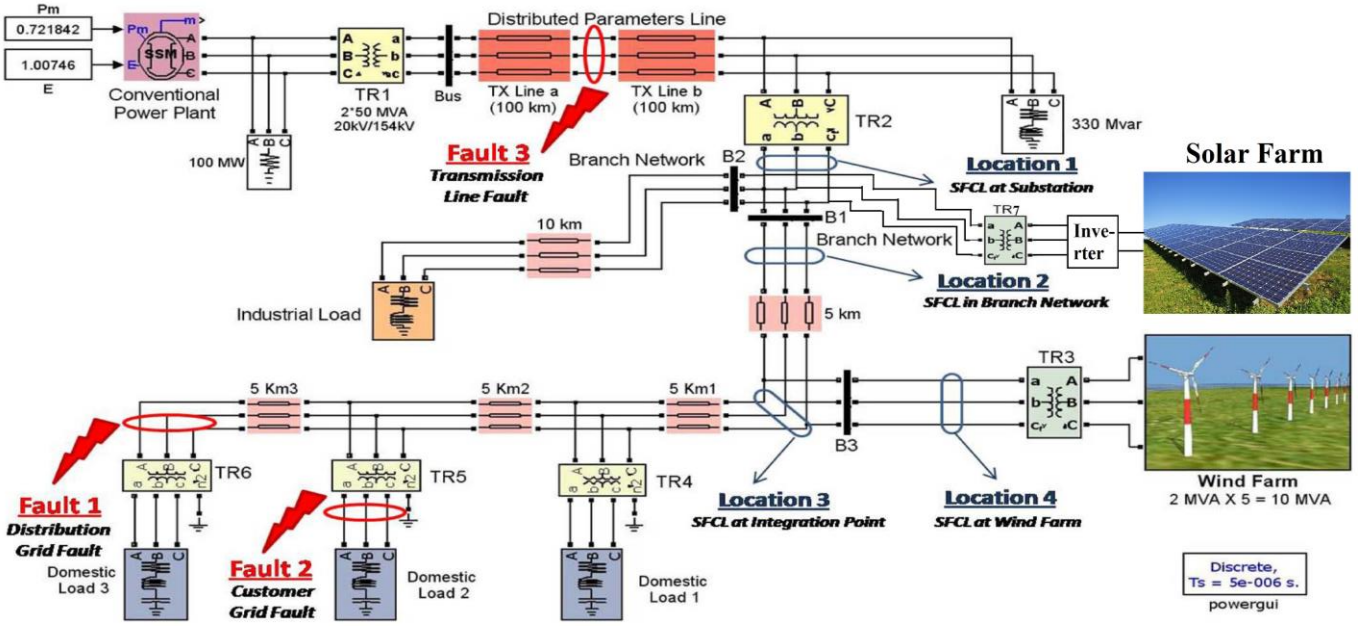

Fig. 11. Power system model designed in Simulink/SimPowerSystem.

V. RESULTS

From simulation study of Power System with both wind farm and solar farm data is compiled in tabular form as given in Tables I-VIII.

TABLE I.
FOR L-L-L-G FAULT: GRID CURRENTS WITHOUT SFCL

Without SFCL	**Fault 1DG**	**Fault 2 CG**	**Fault 3 TL**
Peak Current	2400A	760A	3620A

TABLE II.
FOR L-L-L-G FAULT: GRID CURRENTS WITH SFCL

SFCL Location	***Fault 1DG***	***Fault 2 CG***	***Fault 3 TL***
Location 1	3360A = 40% Increased	1250A = 64.47% Increased	1600A = 54.69% Decreased
Location 2	3360A = 40% Increased	1000A = 34.21% Increased	1450A = 59.11% Decreased
Location 3	820A = 65.83% Decreased	500A = 32.39% Decreased	3500A = 1.1% Decreased
Location 1 & 4	1300A = 45.83% Decreased	700A = 5.26% Decreased	1000A = 72.09% Decreased

TABLE III.
FOR L-L-L FAULT: GRID CURRENTS WITHOUT SFCL

Without SFCL	**Fault 1DG**	**Fault 2 CG**	**Fault 3 TL**
Peak Current	2450A	760A	3650A

TABLE IV.
FOR L-L-L FAULT: GRID CURRENTS WITH SFCL

SFCL Location	***Fault 1DG***	***Fault 2 CG***	***Fault 3 TL***
Location 1	3360A = 40% Increased	1250A = 64.47% Increased	1575A = 56.49% Decreased
Location 2	3360A = 40% Increased	1020A = 33.21% Increased	1458A = 59.72% Decreased
Location 3	820A = 65.83% Decreased	520A = 31.57% Decreased	3620A = 0% Decreased
Location 1 & 4	1300A = 45.83% Decreased	720A = 5.26% Decreased	1010A = 72.09% Decreased

TABLE V.
FOR L-L-G FAULT: GRID CURRENTS WITHOUT SFCL

Without SFCL	**Fault 1DG**	**Fault 2 CG**	**Fault 3 TL**
Peak Current	2400A	760A	3620A

TABLE VI.
FOR L-L-G FAULT: GRID CURRENTS WITH SFCL

SFCL Location	***Fault 1DG***	***Fault 2 CG***	***Fault 3 TL***
Location 1	3360A = 40% Increased	1250A = 64.47% Increased	1575A = 56.49% Decreased
Location 2	3360A = 40% Increased	1000A = 34.21% Increased	1458A = 59.72% Decreased
Location 3	820A = 65.83% Decreased	510A = 32.39% Decreased	3620A = 0% Decreased
Location 1 & 4	1300A = 45.83% Decreased	720A = 5.26% Decreased	1010A = 72.09% Decreased

TABLE VII.
FOR L-G FAULT: GRID CURRENTS WITHOUT SFCL

Without SFCL	**Fault 1DG**	**Fault 2 CG**	**Fault 3 TL**
Peak Current	2400A	760A	3620A

TABLE VIII.
FOR L-G FAULT: GRID CURRENTS WITH SFCL

SFCL Location	***Fault 1DG***	***Fault 2 CG***	***Fault 3 TL***
Location 1	3360A = 40% Increased	1250A = 64.47% Increased	1575A = 56.49% Decreased
Location 2	3360A = 40% Increased	1000A = 34.21% Increased	1458A = 59.72% Decreased
Location 3	820A = 65.83% Decreased	510A = 32.89% Decreased	3660A = 1.1% Increased
Location 1 & 4	1300A = 45.83% Decreased	700A = 5.26% Decreased	1000A = 72.09% Decreased

VI. CONCLUSION

MATLAB Simulink models of grid connected power system consisting of wind farm and solar photovoltaic farm under normal and various faults conditions were presented in this paper. Based on literature survey, it was concluded that that purely resistive SFCL is preferable because it makes the circuit less inductive and provided greater limiting of the initial fault current peak. SFCL model was designed using SimPowerSystem package in MATLAB and was tested successfully for different fault conditions and its results were analyzed in this paper. The strategy location based on technical and economic aspects was found out and suggested through this paper.

REFERENCES

[1] Ok-Bae Hyun, Kwon-Bae Park, Jungwook Sim, Hye-Rim Kim, Seong-Woo Yim, and Il-Sung Oh, "Introduction of a Hybrid SFCL in KEPCO Grid and Local Points at Issue", *IEEE Trans. on Applied Superconductivity*, Vol. 19, No. 3, June 2009.

[2] Lin Ye, Member, M. Majoros, T. Coombs, and A. M. Campbell, "System Studies of the Superconducting Fault Current Limiter in Electrical Distribution Grids", *IEEE Trans. on Applied Superconductivity*, Vol. 17, No. 2, June 2007.

[3] Sung-Hun Lim, Hyo-Sang Choi, Dong-Chul Chung, Yeong-Ho Jeong, Yong-Huei Han, Tae-Hyun Sung, and Byoung-Sung Han, "Fault Current Limiting Characteristics of Resistive Type SFCL Using a Transformer", *IEEE Trans. on Applied Superconductivity*, Vol. 15, no. 2, pp. 2055-2058, June 2005.

[4] Umer A. Khan, J. K. Seong, S. H. Lee, S. H. Lim, "Feasibility Analysis of the Positioning of Superconducting Fault Current Limiters for the Smart Grid Application Using Simulink and SimPowerSystem", *in IEEE Transactions On Applied Superconductivity*, Vol. 21, No. 3, June 2011.

[5] B. C. Sung, D. K. Park, J. W. Park, and T. K. Ko, "Study on a series resistive SFCL to improve power system transient stability: Modeling, simulation and experimental verification", *IEEE Trans. Industrial Electron.*, vol. 56, no. 7, pp. 2412-2419, Jul. 2009.

[6] W. Friedl, L. Fickert, E. Schmautzer, and C. Obkircher, "Safety and reliability for smart-, micro-, and islanded grids, presented at the CIRED Seminar: Smart-Grids for Distribution", Paper 107, Jun. 2008.

[7] J. Driesen, P. Vermeyen, and R. Belmans, "Protection issues in microgrids with multiple distributed generation units", *in Power Conversion Conf.*, Nagoya, April 56 2007, pp. 646-653.

[8] K. Maki, S. Repo, and P. Jarventausta, "Effect of wind power based distributed generation on protection of distribution network", *in IEEE Developments in Power System Protection*, vol. 1, pp. 327-330, Dec. 2004.

[9] L. Dessaint, K. Al-Haddad, H. Le-Huy, G. Sybille, and P. Brunelle, "A power system tool based on simulink", *IEEE Trans. Industrial Electron.*, vol. 46, no. 6, pp. 1252-1254, Dec. 1999.

[10] S. Sugimoto, J. Kida, H. Arita, C. Fakui, and T. Yamagiwa, "Principle and characteristics of a fault current limiter with series compensation", *IEEE Trans. Power Delivery*, vol. 11, no. 2, pp. 842-847, Apr. 1996.

[11] Woo-Jae Park, Byung Chul Sung, Kyung-Bin Song, and Jung-Wook Park, "Parameter Optimization of SFCL With Wind-Turbine Generation System Based on Its Protective Coordination", *IEEE Trans. on Applied Superconductivity*, Vol. 21, no. 3, pp. 2153-2056, June 2011.

[12] Lin Ye, LiangZhen Lin, and Klaus-Peter Juengst, "Application Studies of Superconducting Fault Current Limiters in Electric Power Systems", *IEEE Trans. On Applied Superconductivity*, vol. 12, no. 1, March 2002.

[13] Steven M. Blair, Campbell D. Booth, and Graeme M. Burt, "Current Time Characteristics of Resistive Superconducting Fault Current Limiters", *IEEE Trans. on Applied Superconductivity*, vol. 22, no. 2, April 2012.

[14] J. Kozak, M. Majka, S. Kozak, and T. Janowski, "Comparison of Inductive and Resistive SFCL", *IEEE Trans. on Applied Superconductivity*, vol. 23, no. 3, June 2013.

[15] B. W. Lee, J. Sim, K. B. Park, and I. S. Oh, "Practical Application Issues of Superconducting Fault Current Limiters for Electric Power Systems", *IEEE Trans. on Applied Superconductivity*, vol. 18, no. 2, June 2008.